

Geert Van der Snickt^{1,2,*}, Kathryn A. Dooley³, Jana Sanyova⁴, H  lene Dubois^{4,5}, John K. Delaney³, E. Melanie Gifford³, Stijn Legrand¹, Nathalie Laquiere⁴, Koen Janssens¹

Copyright © 2020
The Authors, some
rights reserved;
exclusive licensee
American Association
for the Advancement
of Science. No claim to
original U.S. Government
Works. Distributed
under a Creative
Commons Attribution
NonCommercial
License 4.0 (CC BY-NC).

INTRODUCTION

In the 1950 to 1951 study, conservation researchers recognized in this cross section the presence of restorers' overpaint, separated from the original paint layers by varnish layers built up in multiple restorations. In their magnified visual and x-ray radiography (XRR) examination of the painting, they also saw evidence of this overpaint in the region of the Lamb's head. However, it was not possible with the techniques available at that time to localize the extent of all the old restorers' overpaint with precision. When faced with insufficient information, conservators and curators err on the side of caution, choosing to leave areas of possible overpaint in place until

*Corresponding author. Email: geert.vandersnickt@uantwerpen.be



Fig. 1. The Ghent Altarpiece by the Van Eyck brothers (1432, Cathedral of Saint Bavo, Ghent, Belgium) with the wings opened. The white rectangle indicates the area featuring the Lamb of God, the central motif of this polyptych and subject of this paper. Color image taken after the 1950s treatment and before the 2019 treatment (© Lukasweb.be - Art in Flanders vzw).

further research provides definitive evidence on their origin. For this reason, along with time limitations, it was decided to remove overpaint only from the area immediately surrounding the head of the Lamb. The result was that in the 1950 to 1951 treatment only, the gilded rays and ears of the original Lamb were uncovered, leading to the unexpected effect of a head with four ears (5).

Since the 1950s, many new in situ analytical tools and data analysis algorithms (6) have been developed and applied to the conservation and study of artworks. Of particular interest here is the development of mobile instrumentation that allows for noninvasive microscale and macroscale chemical imaging directly on the paint surface. The ultimate goal of microscale imaging analysis is to provide virtual cross sections (i.e., the noninvasive mining to obtain stratigraphic and compositional information on the paint layers at any site of the painting) using modalities such as optical coherence tomography (7), confocal elemental mapping (8–10), and femtosecond pump-probe spectroscopy (11). While these methods have shown promising preliminary results, they currently lack sufficient chemical specificity to identify artists' pigments conclusively and, in some cases, show a limited depth or lateral resolution. For the macroscale methods, several are based on imaging spectroscopy (12, 13), the collection of hundreds of narrow spectral band images over a continuous portion of the electromagnetic spectrum. The focus of macroscale methods on spectral information has provided reasonable chemical specificity, but currently, they are without the capability to provide as detailed information about the paint layer structure as cross-sectional methods.

Within the field of conservation science, macro x-ray fluorescence (MA-XRF) imaging (12) and infrared reflectance imaging spectroscopy (RIS) (13) currently are important to art historical scholars and

conservators who seek to document and understand the composition (14), (long-term) chemical reactivity (15), and hidden structure of paintings (16). Infrared RIS and MA-XRF may be regarded as improvements of infrared reflectography (IRR) and XRR, respectively, two (broad spectral band) conventional imaging techniques that are used on a routine basis for the study of paintings and of which the imagery recorded on the *Ghent Altarpiece* is available online (<http://clostertovaneyck.kikirpa.be/>). As illustrated below, the key added value of imaging spectroscopy lies in the fact that many of the constituent artists' materials can be identified in situ and without sampling, and their macroscale distribution can be plotted with high spatial resolution (200 to 750 μm per pixel). The resulting distribution images allow for a direct comparison with visual features on the paint surface such as paint strokes, degradation fronts, and other defects (14, 17). In addition, the penetrative properties of the primary radiation permits probing for subsurface modifications; this can give insight into both the painting process and the restoration history of paintings (12, 13, 16). While MA-XRF and infrared RIS were initially developed separately, it is now becoming clear that their combined use allows for a mutual compensation of the drawbacks of each method (13, 18). That is, each method provides some level of chemical contrast in cases where the other does not. In particular, each technique can reveal materials to which the counterpart is insensitive, for example, overlying layers that strongly attenuate x-rays can prove transparent for infrared radiation and vice versa (16). The implementation of chemical imaging techniques on the macro level can reveal changes in the artistic design, but specifying the specific paint layer(s) in which the artist made modifications is challenging. By comparison, microscale imaging of the paint stratigraphy through paint samples does offer

information on the complex sequence of paint layers—both the work of the original artists and layers of overpaint added by later restorers in the course of almost six centuries—but localized to a specific point (3).

The first phase of the current conservation treatment of the *Ghent Altarpiece*, begun in 2012, focused on the reverse side of the wing panels, which are only visible to the visitor when the altarpiece is closed. During the first phase of treatment, MA-XRF imaging, supplemented with the analysis of a limited number of paint cross-sectional samples, facilitated the identification and accurate localization of extensive overpaints. Combined with historical evidence, this research documented an extensive restoration campaign dating to the middle of the 16th century that encompassed all panels (19). This combined analysis contributed objective chemical evidence to the scholarly debate on conservation treatment decisions. With a much more complete understanding of the extent of overpaints and the state of preservation of the original paint below, it was decided to fully remove these 16th century nonoriginal layers, bringing to light the exquisite quality of the original Eyckian paint surface (20).

Given the success of combining the MA-XRF results with traditional methods (IRR, XRR, and magnified visual examination) during the first treatment phase to map the areas of overpaint, this combined approach was also adopted for the second phase of the conservation program that began in 2016 during which the lower tier of panels on the interior of the altarpiece were treated. It was considered likely that the set of 16th century overpaints identified during the first phase of treatment would also be present on the interior panels. This paper uses the motif of the Lamb of God in the central panel depicting *The Adoration of the Lamb* (fig. S1) to demonstrate the utility of the methods applied in documenting different stages of the painting's history and the results of removing the 16th century overpaint. Because of lingering questions raised during the 1950 to 1951 treatment regarding the remaining overpaint on the Lamb, we sought a more complete understanding of the distribution of the overpaint and a clearer distinction between the overpaint and the original paint structure of the Eyckian Lamb and altar. Thus, both MA-XRF and infrared RIS data were collected and analyzed from the Lamb of God. Although the macroscale chemical imaging provides limited information on stratigraphy, the visualization of material differences helped to separate different painting stages.

RESULTS

MA-XRF and infrared (970 to 1680 nm) RIS image cubes of the Lamb of God and surrounding area were collected with a spatial resolution of 0.75 and 0.17 mm per pixel, respectively. These image cubes were collected in early 2018 before removal of all the 16th century overpaint. From the infrared RIS cube, false-color images were made along with a map of the distribution of basic lead white (hydrocerussite). Elemental maps were extracted from the MA-XRF cube. These new MA-XRF and infrared RIS images provided the required chemical contrast to go beyond the 1950 to 1951 study and begin to assign the extent of the overpaint layers compared to the original Eyckian paint layers. This new chemical imaging data, combined with the conservators' magnified surface examinations, allowed restorers to distinguish between more than one early campaign of restoration. Specifically, the MA-XRF and infrared RIS image products contributed to separating the visual characteristics of the 16th century overpainted Lamb from the Eyckian Lamb, as well as deriving information on how the Eyckian Lamb was painted. To demonstrate this, we pres-

ent images of painted design features such as the head of the Lamb, its body, and the altar: color images made after the 1950s treatment and then after the treatment completed in 2019 (which removed all 16th century overpaint), along with images obtained by spectroscopic analysis.

As noted in Introduction, only some overpaint around the head of the Lamb was removed in the 1950 to 1951 treatment, revealing the original Eyckian ears (color image after 1950s treatment; Fig. 2A) (5, 19, 21). MA-XRF elemental maps displaying the distribution of gold, copper, mercury, and lead are shown in Fig. 2 (C to F), along with a colorized composite of these MA-XRF maps in Fig. 2G. The

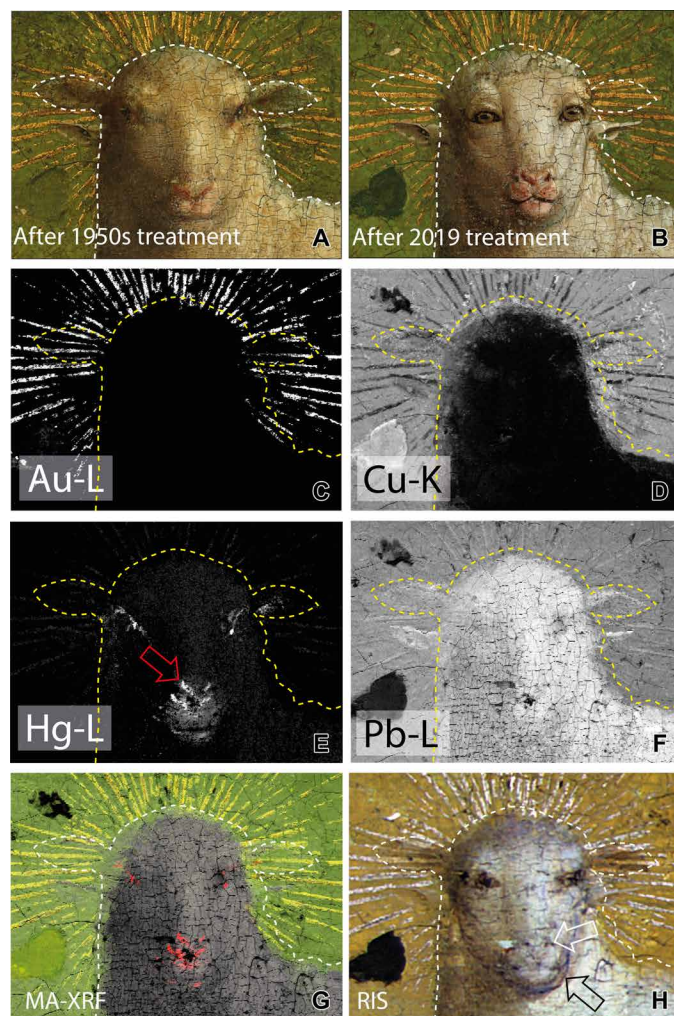


Fig. 2. Detail of the head of the Lamb. Color image (A) before the removal of all 16th century overpaint and (B) after the removal of all 16th century overpaint, revealing the face of the Eyckian Lamb. The dotted lines indicate the outline of the head before treatment (© Lukasweb.be - Art in Flanders vzw). MA-XRF elemental maps showing the distribution of (C) gold, (D) copper, (E) mercury with a red arrow indicating the position of the Eyckian Lamb's nostrils and (F) lead. (G) Colorized composite MA-XRF elemental map showing the elemental distribution of copper (in green), mercury (in red), gold (in yellow), and lead (in gray). (H) Composite false-color infrared RIS image (B, 1000; G, 1350; R, 1650 nm) shows underdrawn lines, indicating the position of the facial features of the Eyckian Lamb. The white arrow indicates the nostrils, whereas the black arrow indicates the jawline. All chemical images were collected after varnish removal but before 16th century overpaint removal.

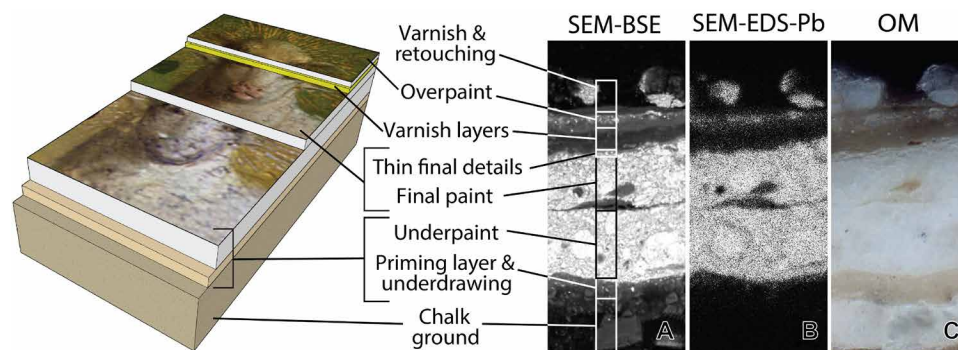


Fig. 3. Paint microsample extracted from the body of the Lamb. The scheme on the left illustrates the stratigraphy observed in the paint cross section collected in 1950 to 1951 and reanalyzed here. An area of the cross section is shown on the right, recorded with three different methods (from left to right): (A) Backscattered electron image recorded with a scanning electron microscope (SEM-BSE) and (B) lead distribution image recorded with an SEM equipped with an energy dispersive x-ray spectrometer (SEM-EDS-Pb), followed by (C) an optical microscopy (OM) image. The uppermost “varnish and retouching” layer, but not the overpaint, was removed before imaging spectroscopy was done. Size of micrographs: 95 μm by 42 μm .

corresponding false-color infrared RIS image is shown in Fig. 2H. The outline of the overpainted head of the Lamb, as it appeared before the recent removal of the 16th century overpaint, is shown as a dashed line. This makes it clear that the copper paint of the green meadow extends inside the outline of the Lamb’s head. To produce a clean edge of the head of the Lamb against the green meadow, standard Netherlandish painting practice in the 15th century dictated that the copper green underpaint would have extended into the area planned for the head, later to be covered by the final white paint of the Lamb (Fig. 2, D and F). After completion of the Lamb, the artist’s final touch was the gilded rays of the halo applied right up to the contour of the Lamb’s head and ears. The gold distribution in the elemental map (Fig. 2, C and G) shows that the rays continue inside the dotted line on the right-hand side and are also situated underneath the paint depicting the upper set of ears. These findings demonstrate that the restorer’s 16th century overpaint enlarged the Lamb’s head along the right side of the neck and shoulder and also added the upper ears. The false-color infrared RIS image (Fig. 2H) shows similar information, as the background (light brown color) extends inside the dotted line on the right-hand side, and the rays of the halo are present underneath the upper set of ears. The MA-XRF and RIS chemical images show that the gold rays are not present underneath the lower set of ears but instead were applied only up to the outer edges of those ears.

The MA-XRF map for mercury (Fig. 2, E and G), an element associated with the red pigment vermilion (HgS), reveals the presence of two sets of nostrils that are roughly v-shaped. The lower set aligns with the nostrils of the Lamb with the 16th century overpaint (Fig. 2A), whereas the upper set (red arrow in Fig. 2E) is smaller and coincides with dark underdrawing “dots” (Fig. 2H, white arrow), likely associated with the Eyckian Lamb. In the infrared RIS image, dark lines of the preparatory underdrawing that delineate the division between the lips and the jawline (Fig. 2H, black arrow) are also visible. In addition, in the infrared RIS image, design features from two sets of eyes can be seen. Dark, irregularly shaped spots align with the pupils of the overpainted eyes. Comparison with the mercury map shows that vermilion also is likely associated with the overpainted eyes. The other set of eyes is characterized in the infrared RIS image by some drawing lines and dark pupils and is slightly lower on the face. In contrast to the outward-looking eyes of the Lamb depicted in the

16th century overpaint, this set looks forward toward the viewer. Collectively, these facial features indicate that the Eyckian face of the Lamb had forward-gazing eyes and effectively a shorter muzzle than the 16th century restorer’s overpainted face. During the recent conservation treatment that was completed in 2019, conservators were able to safely remove the 16th century overpaint that completely obscured the head and patches of the body in the Lamb of God. The head of the Lamb that emerged (Fig. 2B) has many of the facial features that previously could be elucidated from analysis of the chemical imaging data.

In the 1950 to 1951 study, evidence for overpaint on the body of the Lamb came most conclusively from a paint cross section (Fig. 3) extracted from the Lamb’s body, of which the location is identified in Fig. 4A. The results from reexamination of this cross section by means of optical microscopy (OM) and scanning electron microscopy with energy dispersive x-ray spectroscopy (SEM-EDS) analysis confirmed many of the findings from the 1950s analysis. In summary, the stratigraphy consists of a chalk ground, priming layer, and two thick applications of lead white-based paint (corresponding to the underpaint and final paint of the Eyckian Lamb), as well as thin traces of a discontinuous third lead white layer (newly reported here) that may correspond to final details such as the curls of the fleece. The absence of dirt and varnish in between these strata strengthens the hypothesis that these layers were applied within only a short interim and, thus, likely were painted by the Van Eyck brothers. On top of the Eyckian paint layers, several thick varnish layers are present, which must have originated in multiple restorations, followed by a series of interleaved layers of overpaint (rich in lead white) and more varnish.

The contrast seen in MA-XRF and infrared RIS images derives from differences in chemical composition. However, since the paint cross section from the body of the Lamb (Fig. 3) confirms that it was both painted and overpainted using superimposed layers of lead white, the information obtained from MA-XRF was expected to be limited because the high x-ray absorption coefficient of lead restricts the depth information that can be obtained. In contrast, infrared RIS has a more extended penetration depth in lead white-rich paints. The absorption coefficient of lead white is negligible in the visible and infrared spectral regions; however, its scattering coefficient, while large in the visible, decreases markedly at infrared wavelengths. The

differences in penetration of the lead white-rich layers can be seen in Fig. 4 (C to F), which compare the MA-XRF elemental maps and the false-color infrared RIS of the entire Lamb.

In the body of the Lamb, the lead map (Fig. 4C) shows the same shape of the animal as seen in the image before removal of 16th century overpaint (Fig. 4A); the intensity variation also appears to show denser areas of lead white corresponding to the final details of curly fleece. Because RIS was restricted to the infrared spectral region, better transmission of light through the paint layers was expected, the latter including any overpaint, final, and underpaint layers. Compared to the MA-XRF maps (Fig. 4, C to E) and the image before removal of all 16th century overpaint (Fig. 4A), the false-color infrared RIS image (Fig. 4F) shows a slightly smaller form of the Lamb's body that appears opaque, as well as a translucent, thinly painted region along the back and hindquarters. Further evidence

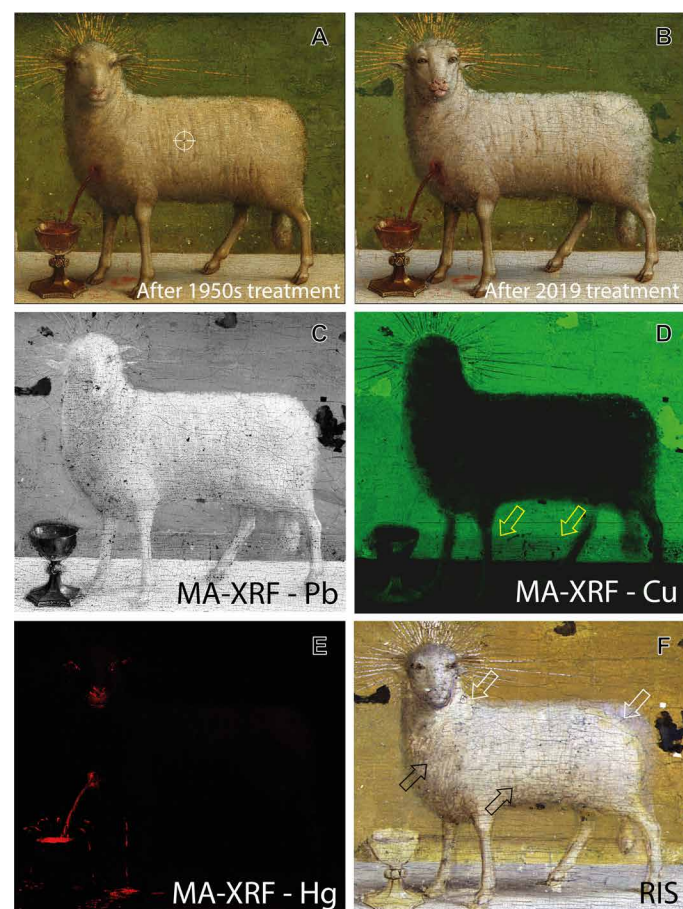


Fig. 4. The Lamb of God. (A) Color image of the Lamb before removal of all 16th century overpaint; the location of the paint sample discussed in Fig. 3 is indicated by a white reticle. (B) The Lamb after removal of all 16th century overpaint in 2019 (© Lukasweb.be - Art in Flanders vzw). (C to E) MA-XRF elemental maps recorded before removal of all 16th century overpaint showing the distribution of (C) lead (in white), (D) copper (in green), and (E) mercury (in red). The yellow arrows in (D) indicate the edge of the larger altar. (F) False-color infrared RIS image (B, 1000; G, 1350; R, 1650 nm) revealing underdrawing that denotes the size of the smaller version of the Eyckian Lamb's back and tail, more rounded hindquarters, repositioning of the hooves, and the larger size of the altar. The white arrows indicate underdrawing lines defining a smaller body, whereas the black arrows point to wavy underdrawing lines applied for torso modelling and fleece texture.

for these changes to the size of the Lamb can be seen in principal component images from the RIS data (see fig. S8), although such images rarely represent contributions from a single pigment. A focus on the spectral features that directly relate to pigments used in the Lamb is discussed further below. The false-color infrared RIS image also shows the presence of underdrawing, including lines that define the smaller, opaque body (white arrows, Fig. 4F) and “wavy” brown lines used to model the Lamb's torso and suggest the texture of the fleece (black arrows). The brown lines are most apparent on the Lamb's chest and underside of the belly. The lines are not present in the images before or after 16th century overpaint removal in Fig. 4 (A and B), suggesting that they are below the surface and are likely underdrawing. Also, visible in the false-color infrared RIS image are underdrawing lines that denote the legs and hooves of the Lamb. Whereas some of the lines are brown (near the Lamb's tail), others are wider, black lines (such as that delineating the front of the proper left front leg) that are visually similar to the black underdrawn line that reinforces the jawline of the Eyckian Lamb in Fig. 2H.

The difference between these two drawing types (thinner brown lines or thicker black lines) can be better understood by looking at a detail from the angel to the left of the Lamb (Fig. 5). Infrared RIS can be used to distinguish between different underdrawing materials owing to changes in their absorption and scattering coefficients as a function of wavelength in the infrared. This can only be exploited by using hundreds of narrow spectral bands, as is done in RIS. In contrast, since broad spectral band traditional IRR is the sum of all these spectral bands, the ability to distinguish artist materials is substantially limited. In the IRR image (Fig. 5B), the underdrawing lines are only distinguishable based on their relative intensity. The false-color infrared RIS image (Fig. 5C) shows two types of underdrawing materials. One type consists of thin, brownish lines that appear to have been rendered using a fine brush and a liquid medium (Fig. 5C, brown arrows). The other type is thicker, black lines that

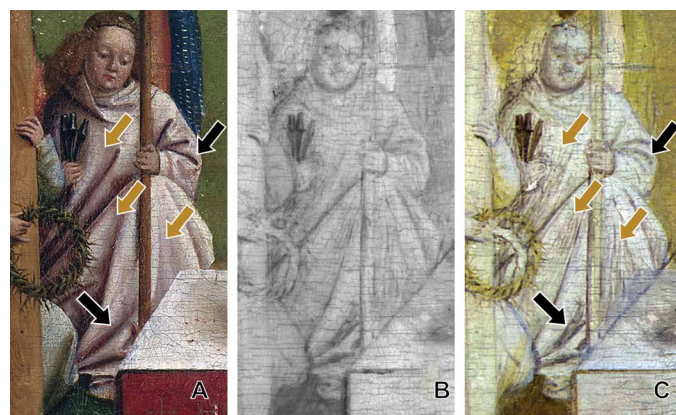


Fig. 5. Detail of the angel to the left of the Lamb. (A) Color image after 2019 cleaning and during retouching (© Lukasweb.be - Art in Flanders vzw). The brown and black arrows indicate the position of the underdrawing lines shown in (C). (B) IRR image (http://clostertovaneyck.kikirpa.be, © KIK-IRPA, Brussels) revealing the infrared-absorbing underdrawing. (C) The corresponding false-color infrared RIS image (B, 1000; G, 1350; R, 1650 nm) allows further distinction of the types of underdrawing: (i) Brown arrows indicate the finer lines of the first stage of underdrawing, which appear brownish in the RIS image, and (ii) black arrows show the thicker lines in a liquid medium from the second stage of underdrawing, which appear blackish in the image. The yellow color in the background is a result of partial penetration of copper-containing green paint in the infrared.

were likely more heavily applied, also in a liquid medium (Fig. 5C, black arrows). These two types of underdrawing are clearly also present in the Lamb (Figs. 2H and 4F). Together, these results indicate that the infrared RIS image is dominated by the underdrawing, priming layer, and underpaint layer of the Eyckian Lamb.

As seen in the infrared RIS image of the Lamb in Fig. 4F, a sharp, crisp boundary is not observed between the light brown background (corresponding to the green meadow) and the white Lamb along the back and hindquarters. Instead, this area appears as a translucent, hazy white that is clearly on top of the light brown background. Underdrawing lines are present at the top of the hindquarters and along the neck and shoulder (Fig. 4F, white arrows) and are found along the boundary between the opaque and hazy translucent white paint. This suggests that there was a version of the Lamb that had a more naturalistic build with a slightly sagging back and more rounded hindquarters.

The MA-XRF copper map shown in Fig. 4D indicates that changes were made to the altar as well. The areas of lower intensity of copper along the back edge of the altar coincides with an underdrawing line seen in traditional IRR images, also visible in the false-color infrared RIS image in Fig. 4F. A larger section of the infrared RIS false-color image (Fig. 6A) shows the extent of the underdrawing of the altar. The drawn altar was deeper and with a slightly different perspective than the final painted altar, indicated by the edge of the white plane that extends beyond the drawing lines on the left and right. The abandoned part of the altar is characterized by having a lower copper intensity and higher reflectance intensity, which suggests the change occurred during a paint campaign and not directly after the underdrawing was completed. To confirm that the deeper altar was painted,

the reflectance spectra from different areas on the altar were examined. The paint of the altar is rich in lead white as indicated by the MA-XRF lead map (Fig. 4C) and the presence of a strong hydroxyl absorption feature at 1446 nm in the RIS spectra, indicative of basic lead white (hydrocerussite) (Fig. 6B, blue and green spectra). The finished altar likely consists of two paint layers containing lead white: the underpaint and the final paint. The depth of the 1446-nm feature is indicative of the amount of basic lead white present and is most pronounced in the upper (blue) spectrum of Fig. 6B. In contrast, the average spectrum from the green meadow (Fig. 6B, yellow spectrum) shows that much less lead white is present, along with a broad absorption from ~967 to 1375 nm, indicative of copper green pigments. In this region of the green meadow, the contribution from lead white may be from small amounts of lead white added to the green paint of the meadow or in the priming layer. The average reflectance spectrum from the abandoned region of the altar (Fig. 6B, red spectrum) has an absorption feature at 1446 nm whose depth is less than that of the finished altar but greater than that of the green meadow, indicating that at least the underpaint layer of the altar extended to the underdrawn line. This suggests that the larger drawn altar was underpainted with lead white before it was abandoned. This is consistent with the MA-XRF Cu image in Fig. 4D revealing a less intense copper signal, likely from a thinner build-up of green paint in this area (as indicated by the yellow arrows).

The paint of the Lamb itself is mostly dominated by lead white, including the overpaint. The expected stratigraphy of the Eyckian Lamb is composed of an underpaint layer and a final paint layer whose thicknesses are much larger than the overpaint layers (see cross section in Fig. 3). A map derived from RIS data indicating the integrated area of the hydroxyl absorption at 1446 nm was obtained by fitting each reflectance spectrum in the image cube with a convex hull function, the intensity of the resulting map (Fig. 6C) being proportional to the amount of basic lead white present. In comparison to the 16th century overpainted Lamb (Fig. 4A), the lead white map clearly shows the more naturalistic shape of the Lamb's sagging back, rounded hindquarters, smaller tail, and the larger altar.

Duly informed by the MA-XRF and infrared RIS imagery, as well as by extensive magnified examination of the paint surface, the second phase of conservation treatment of the *Ghent Altarpiece* undertook the complete removal of the 16th century (and later) overpaint, as shown in the resulting images of the Lamb in Figs. 2B and 4B. This resulted in changes to the Lamb's face that had many of the facial characteristics identified with the MA-XRF and infrared RIS analysis. The body of the Lamb retained the same shape as the image before 16th century overpaint removal. The difference between the body of the Lamb after removal of the 16th century overpaint (Fig. 4B) and the body recovered from the infrared RIS analysis here (Fig. 6C) indicates that the lead white paint layer used to define the larger squared-off hindquarters was applied before the 16th century restoration.

An interesting question is whether this layer was applied during the Eyckian painting process or at some later time. After removal of the 16th century overpaint, two observations suggest that the paint may have been applied after a smaller version of the Lamb was painted with a high degree of finish and possibly considered completed. This small Eyckian Lamb would likely have been considered finished once the fine, tight curls of the fleece were applied. One observation comes from visual examination of the paint, and the other comes from examination of the x-radiograph. Close visual examination of the paint

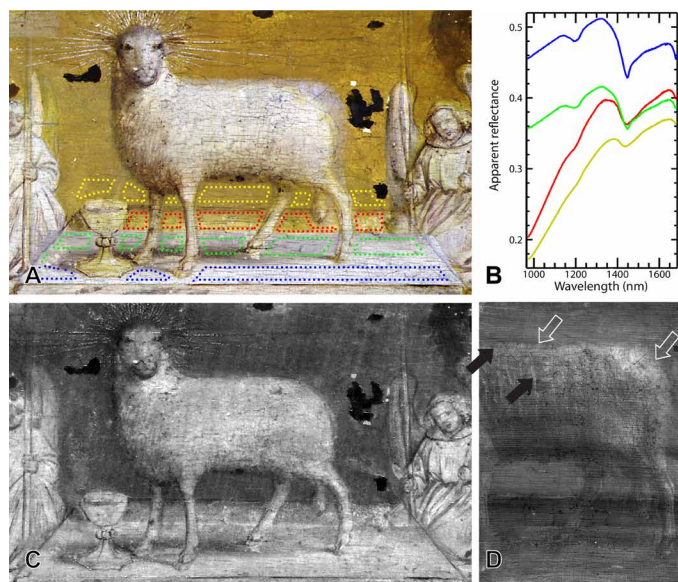


Fig. 6. RIS images and map of the Lamb derived from processing the infrared reflectance image cube. (A) Infrared RIS false-color image (B, 1000; G, 1350; R, 1650 nm) and (B) associated average infrared RIS spectra collected from the colored dashed shapes shown in (A). (C) RIS lead white map derived from processing the infrared RIS image cube. Brighter areas of the map indicate stronger absorption from the -OH group of lead white. (D) X-ray radiograph detail (<http://clostertovaneyck.kikirpa.be>, © KIK-IRPA, Brussels) after removal of all 16th century overpaint in 2019. The white arrows indicate where the body of the Lamb was revised, whereas the black arrows point to fleece texture.

surface shows that the texture of the added paint extending the upper contour of the Lamb's back and hindquarters differs substantially from the paint in the center of the body. The x-radiograph shows vertical "fuzzy" columns of opaque paint (Fig. 6D, lower black arrow) that are likely from the curls of the fleece, and these curly features end at a thin horizontal opaque ridge, which corresponds with the upper contour of the small Eyckian Lamb (Fig. 6D, upper black arrow). Outside of that upper contour, the x-radiograph shows an additional zone of thin, opaque paint (white arrows), which coincides with the translucent, hazy white revision shown in the infrared RIS image (Figs. 4F and 6A). Magnified examination of the paint surface confirms that the paint used to revise the Lamb to give it squared-off hindquarters shows less finesse in its application: It was dabbed on in a single tone of white paint, without the surface variations that define the texture of the fleece. Together, these observations support the hypothesis that the small Eyckian Lamb had the boundaries shown in the infrared RIS lead white map (Fig. 6C) and that this highly finished version was subsequently reworked to modify the shape of the Lamb's body.

DISCUSSION

The combination of two imaging spectroscopic techniques, MA-XRF and infrared RIS, allowed studying the painting process of the Lamb of God with chemical specificity. In summary, the combined results established the presence of three versions of the Lamb: a first, highly finished, small Eyckian version, a second version whereby the hindquarters were enlarged and squared off (revealed after overpaint removal), and a third, 16th century version that extensively modified the head but respected the shape of the body from the second version. The second version could have been either a very late change by the original artist(s) or an early intervention by another painter. This identification of three versions is strengthened when historical information and conservation treatment details are integrated with the chemical imaging results.

The known drawing and painting style of the Van Eyck brothers can be used to further support the assignment of what was above referred to as the small Eyckian Lamb. The Van Eyck style of underdrawing is characterized by a first stage of fine lines that define design features as well as parallel hatching (rather than cross-hatching) to model the forms and a second stage of heavier lines that reinforce or revise the forms (22, 23). This characteristic drawing style is clearly seen in the angels (see Fig. 5). In the Lamb, the wavy parallel hatching that models the body while also evoking its fleece is characteristic of the first Van Eyck drawing stage. In the legs, both drawing stages can be seen. The dark underdrawing lines in the face appear characteristic of the second stage. The drawing defining the shoulder and the rounded hindquarters is narrow and possibly associated with the first drawing stage, but the drawing stage is difficult to conclusively categorize because the drawing is covered by lead white paint and likely overlaps with the copper paint of the green meadow. An important characteristic of the Van Eyck painting style is the finesse for which they render final details. Thus, the finding of the curly fleece only within the boundaries of the smaller Lamb is consistent with it having been painted by the Van Eyck brothers.

There are some other painted and drawn features revealed by the chemical imaging analysis that are unexpected, such as the forward-looking eyes of the Lamb and the change in the size and perspective angle of the top of the altar. The interpretation of the forward-looking

eyes is part of an ongoing, unpublished scholarly debate (24). Some scholars have proposed that the Lamb was deliberately rendered less true to life to obtain a more intense and confronting appearance. Since the Lamb is an embodiment of Christ, the forward-gazing eyes could have a religious connotation. A simpler explanation may be that the painting of animals with forward-facing eyes is typical of an older style that was still present in the 15th century but disappeared as artists mastered a more naturalistic depiction of animals. The team treating the altarpiece noted that animals with both forward- and outward-looking eyes are seen in the panels of the *Ghent Altarpiece*. For example, in the panel of *The Just Judges* (stolen in 1934 but documented in photographs), there are horses with eyes that look forward, whereas in the panel of *The Knights of Christ*, the horses are depicted more naturalistically with outward-looking eyes. Thus, it is not unexpected that the Van Eyck brothers would have painted the Lamb with forward-facing eyes that directly engage the viewer.

Chemical imaging also revealed that the planned larger altar was at least painted with an underpaint layer of lead white and then abandoned before completion of the painting. Supporting this is a report on the presence of white paint beneath the green paint in the abandoned section of the altar determined from optical stereomicroscopy (25). This change was likely made by the Van Eyck brothers during the painting process. This is not surprising since there is ample evidence for many changes to the design that were made during the painting process and so were not indicated in the drawing. This design change may have been made for two reasons. Looking at the position of the small Eyckian Lamb on the originally planned altar in Fig. 6C, the Lamb is not centered along the depth direction of the altar, which makes it seem unbalanced. To correct for this, the depth of the altar was reduced. This also results in another benefit in that it provides more space between the altar and the nearby angels. The infrared RIS images also show that the edges of the altar were revised in paint to effectively change the tilt of the altar, as has been noted in the previous study (25). Because Netherlandish painters at this time did not use vanishing points to define the perspective but instead rendered three-dimensional objects intuitively, the change in the tilt of the altar may have been done to make the design more pleasing.

After the removal of the 16th century overpaint by mechanically shearing it from the thick buildup of old varnish (as seen in the paint cross section in Fig. 3), it became clear that the enlargement of the Lamb was done in paint applied over the green meadow. The research here cannot definitively establish whether this paint is a change (pentimento) by the original artist(s) or a very early restoration. There is evidence for very old damages that precede the 16th century overpainting campaign (21). One clue that has emerged is the observation that this paint lacks the texture and detail expected for Eyckian paint. However, because the material evidence available at the time of the current conservation treatment could not establish whether this was original paint or an early restoration, the enlarged contour of the Lamb was not removed. From the early 19th century, there has been an ongoing scholarly debate on the respective contributions of the two brothers, Hubert and Jan Van Eyck (26). Here, too, the material evidence currently available does not allow conclusions to be drawn.

From a more technical point of view, the added value of MA-XRF and infrared RIS with respect to conventional XRR and IRR was demonstrated in this research. In particular, the element specificity of MA-XRF imaging permitted examining the complex structure and

composition in a more selective way as compared to XRR. Whereas XRR cannot distinguish between heavy elements like lead and mercury, MA-XRF permits identifying and mapping chemical elements separately, which enabled the visualization of the nostrils of the Eyckian Lamb underneath the 16th century overpainted Lamb. In an analogous way, classic IRR can detect a variety of different IR-absorbing materials, such as carbon black, umber, or copper pigments, but cannot distinguish among them. Infrared RIS makes use of the materials' different spectral signatures, which allowed for the separation between two underdrawing campaigns, as well as a separation of copper pigments from lead white. The spectral information provides the capability to discriminate among artists' materials.

The sensitivity of MA-XRF and infrared RIS to distinguish and map pigments is not the same and varies with the pigments used and the paint layering structure. Using both methods together, these differences can be exploited for a more robust and comprehensive identification and mapping of pigments in layered structures. For both modalities, the degree of depth penetration depends on the absorbance and scattering properties of the pigments within the paint layers. Both modalities helped to visualize the facial features of the Eyckian Lamb. The MA-XRF map of mercury (associated with vermilion) showed the placement of the nostrils, whereas infrared RIS revealed the infrared-absorbing underdrawing in the face, as well as the boundary between the copper green landscape and the lead white associated with the head and neck of the Lamb. Together, these maps and images provided the shape and position of the key facial features that defined the head and neck of the Eyckian Lamb.

In conclusion, we have demonstrated that the combination of infrared RIS and MA-XRF, now in the vanguard of heritage science, expands our possibilities for resolving complex conservation and art historical issues. These imaging technologies can be used to predict the characteristics of specific painted features before the removal of overpaint. Combined with the conservators' thorough optical examination informed by years of experience and insights derived from paint cross sections, chemical imaging methods will no doubt be central to furthering interdisciplinary research and contributing to resolving art historical and theological issues on the *Ghent Altarpiece* and other works of art.

MATERIALS AND METHODS

The chemical imaging campaign was divided into two phases and done in the conservation studio. First, the entire panels were imaged with an in-house MA-XRF scanning instrument. Next, the ensuing elemental distribution maps were used to define areas of interest, such as the Lamb of God, that would benefit from complementary infrared RIS experiments. All chemical images discussed in this work were collected in the early stages of the conservation treatment, when only the surface varnish had been removed.

Macroscopic x-ray fluorescence imaging

The MA-XRF instrument (fig. S2) is an optimized variant of the very first mobile MA-XRF setup, built and described by Alfeld *et al.* as "Instrument B" (27). The measurement head consists of a 50-W XOS Xbeam micro tube with Mo anode (XOS, USA) operated at 50 kV and 1 mA and one Vortex EX-90 SDD detector with an active area of 50 mm² positioned at 45° relative to the surface normal. The excitation beam was normal to the painting surface and was focused to a focal spot of ca. 50 μm by means of a polycapillary x-ray lens.

This measurement head is mounted on a software-controlled X-Y motor stage with a maximum travel range of 57 cm by 60 cm. MA-XRF scans were performed by sweeping the measuring head systematically over the paint surface at a constant speed. Careful positioning and alignment of the scanner ensured that the detector remained ca. 1 cm away from the panel painting. Retaining this constant instrument-to-painting distance maintained the anticipated spot size and prevented fluctuation of the attenuation of the x-ray fluorescence signals in ambient air. During the movement, the detector was read out every 200 ms, which, given the scan speed of ca. 3.75 mm/s, gave a collection footprint of ca. 0.75 mm × 0.75 mm for each pixel in the image cube. The resulting spectral data cube was processed through dynamic analysis using the bAxil (28) software package. The grayscale of the resulting images is linear to the detected intensities. However, after spectral deconvolution, the levels in the histogram of each individual image were manually moved or stretched to optimize contrast and readability by means of the Datamuncher software (29).

Reflectance imaging spectroscopy

Infrared reflectance image cubes were collected with a line-scanning imaging spectrometer (modified SOC-720SWIR, Surface Optics Corp., CA, USA) shown in fig. S3 that uses a transmission grating prism spectrometer and a 640 × 512-pixel InGaAs focal plane array (640SDV-1.7RT, Sensors Unlimited, NJ, USA). The line-scanning imaging spectrometer has optimal signal-to-noise ratio from 967 to 1680 nm, with a spectral sampling of 3.4 nm, resulting in 209 spectral bands. The painting was illuminated with two lamps containing 125-W quartz halogen bulbs (Lowel Pro-light with Impact 3000 K FSH bulb) placed at ±45° to the surface normal. A rheostat was used to adjust the intensity of the lights to be no more than 1000 lux at the surface of the artwork. Image cubes were collected at an integration time of 33 ms per line, and the line field of view was changed by rotation of a scan mirror positioned at the front of the optical system. The spatial sampling at the artwork was 0.17 mm per pixel. The dark current was subtracted from the image cubes, and non-uniformities in illumination were corrected by dividing by a dark-subtracted image cube of a diffuse reflectance standard (99% reflector, 30 cm by 30 cm Spectralon panel, Labsphere, NH, USA). This procedure also converted the cubes to relative reflectance. The 14 reflectance image cubes collected in the region of the Lamb were then mosaicked and registered using a point-based algorithm to spatially align the cubes to a reference color image (30). The false-color images shown in the paper were created by placing the spectral band images specified into the red, green, and blue color channels of an RGB color image. Maps displaying the distribution of lead white were calculated from the reflectance image cube by integrating the area of a characteristic absorption at 1446 nm.

Optical microscopy and scanning electron microscopy with energy dispersive x-ray spectroscopy

The microscopic paint sample presented in this paper was taken from the Lamb during the previous conservation treatment in 1950 to 1951. The sample was embedded in acrylic resin and cross-sectioned to allow for detailed study of the layer structure and pigment composition. During the present campaign, the cross section, still available in the laboratory archive of the Royal Institute for Cultural Heritage (KIK-IRPA), was repolished and reexamined. It was first observed with OM using a polarizing light microscope on an Axio Imager M1

(Carl Zeiss, Oberkochen, Germany) with ultraviolet illumination (excitation band-pass filter from 390 to 420 nm) at magnifications up to $\times 500$. Subsequently, the pigment compositions of the ground and paint layers were analyzed by means of SEM-EDS on a Zeiss EVO LS15 microscope with backscattered electron (BSE) and EDS detectors (Oxford Instruments X-MaxN 80 mm², AZtec Oxford Instruments Software). EDS analyses were run at an acceleration voltage of 15 kV. Analytical results were correlated with the optical images and the MA-XRF elemental distribution images, permitting a more accurate interpretation of the MA-XRF maps.

Infrared reflectance reflectography

The broadband infrared reflectogram was collected using a Lion Systems IRR camera, equipped with an InGaAs detector having a 640×512 -pixel focal plane array and a spectral response of 1100 to 1700 nm. A micro-Nikkor 55-mm lens, fitted with a narrow bandwidth filter of 1500 to 1730 nm was mounted on the camera. The camera was moved by a motorized stage that maintained a constant distance between the lens and the painting surface, compensating for any warping in the wooden panel. Individual IRR images, each recording an area of 5 cm by 4 cm on the paint surface, were digitally assembled into larger images via Adobe Photoshop. Lighting was provided by two freestanding halogen lights, one placed at either side of the painting.

X-ray radiography

XRR images were taken using a Baltospot 110 generator from Balteau NDT using a 50-kV voltage and a current of 12 mA. AGFA Structurix D4 analogue x-ray film strips of 35-cm wide were cut to the desired length and placed against the painted side of the panels. The generator was positioned at a distance of 7 m from the artwork, and the film was irradiated for 10 min. After exposure, the films were developed and digitized using a high-resolution Laser Film Digitizer (Array Corporation, 2905HD). The resulting digital images were assembled using Adobe Photoshop software.

SUPPLEMENTARY MATERIALS

Supplementary material for this article is available at <http://advances.sciencemag.org/cgi/content/full/6/31/eabb3379/DC1>

[View/request a protocol for this paper from Bio-protocol.](#)

REFERENCES AND NOTES

1. S. Muñoz Viñas, *Contemporary Theory of Conservation* (Butterworth-Heinemann, 2005).
2. P. Coremans, La technique des "Primitifs flamands": Etude scientifique des matériaux, de la structure et de la technique picturale. III. Van Eyck: l'Adoration de l'Agneau Mystique (Gand: Cathédrale Saint-Bavon). *Stud. Conserv.* **1**, 145–161 (1954).
3. J. Plesters, Cross-sections and chemical analysis of paint samples. *Stud. Conserv.* **2**, 110–157 (1956).
4. P. Coremans, R. J. Gettens, J. Thissen, La technique des "Primitifs flamands". *Stud. Conserv.* **1**, 1–29 (1952).
5. P. Coremans, *L'agneau Mystique au Laboratoire: Examen et Traitement* (De Sikkel, 1953).
6. Z. Sabetsarvestani, B. Sober, C. Higgit, I. Daubechies, M. R. D. Rodrigues, Artificial intelligence for art investigation: Meeting the challenge of separating X-ray images of the *Ghent Altarpiece*. *Sci. Adv.* **5**, eaaw7416 (2019).
7. P. Targowski, M. Iwanicka, M. Sylwestrzak, C. Frosinini, J. Striova, R. Fontana, Using optical coherence tomography to reveal the hidden history of *The Landsdowne Virgin of the Yarnwinder* by Leonardo da Vinci and studio. *Angew. Chem. Int. Ed. Engl.* **57**, 7396–7400 (2018).
8. I. Reiche, M. Eveno, K. Müller, T. Calligaro, L. Pichon, E. Laval, E. Mysak, B. Mottin, New insights into the painting stratigraphy of *L'Homme blessé* by Gustave Courbet combining scanning macro-XRF and confocal micro-XRF. *Appl. Phys. A* **122**, 947 (2016).
9. A. R. Woll, J. Mass, C. Bisulca, M. Cushi-Nan, C. Griggs, T. Wanz, N. Ocon, The unique history of the *Armorer's Shop*: An application of confocal X-ray fluorescence microscopy. *Stud. Conserv.* **53**, 93–109 (2008).
10. T. Lachmann, G. van der Snickt, M. Haschke, I. Mantouvalou, Combined 1D, 2D and 3D micro-XRF techniques for the analysis of illuminated manuscripts. *J. Anal. At. Spectrom* **31**, 1989–1997 (2016).
11. T. E. Villafana, W. P. Brown, J. K. Delaney, M. Palmer, W. S. Warren, M. C. Fischer, Femtosecond pump-probe microscopy generates virtual cross-sections in historic artwork. *Proc. Natl. Acad. Sci. U.S.A.* **111**, 1708–1713 (2014).
12. J. Dik, K. Janssens, G. Van der Snickt, L. van Der Loeff, K. Rickers, M. Cotte, Visualization of a lost painting by Vincent van Gogh using synchrotron radiation based X-ray fluorescence elemental mapping. *Anal. Chem.* **80**, 6436–6442 (2008).
13. K. A. Dooley, D. M. Conover, L. D. Glinsman, J. K. Delaney, Complementary standoff chemical imaging to map and identify artist materials in an early Italian Renaissance panel painting. *Angew. Chem. Int. Edit.* **53**, 13775–13779 (2014).
14. K. A. Dooley, E. M. Gifford, A. van Loon, P. Noble, J. G. Zeibel, D. M. Conover, M. Alfeld, G. Van der Snickt, S. Legrand, K. Janssens, J. Dik, J. K. Delaney, Separating two painting campaigns in *Saul and David*, attributed to Rembrandt, using macroscale reflectance and XRF imaging spectroscopies and microscale paint analysis. *Herit. Sci.* **6**, 46 (2018).
15. S. A. Centeno, C. Hale, F. Carò, A. Cesaratto, N. Shibayama, J. K. Delaney, K. A. Dooley, G. Van der Snickt, K. Janssens, S. A. Stein, Van Gogh's *Irises and Roses*: The contribution of chemical analyses and imaging to the assessment of color changes in the red lake pigments. *Herit. Sci.* **5**, 18 (2017).
16. G. Van der Snickt, S. Legrand, I. Slama, E. Van Zuin, G. Gruber, K. Van der Stighelen, L. Klaassen, E. Oberthaler, K. Janssens, In situ Macro X-ray fluorescence (MA-XRF) scanning as a non-invasive tool to probe for subsurface modifications in paintings by P.P. Rubens. *Microchem. J.* **138**, 238–245 (2018).
17. K. Janssens, G. Van der Snickt, M. Alfeld, P. Noble, A. van Loon, J. Delaney, D. Conover, J. Zeibel, J. Dik, Rembrandt's 'Saul and David' (c. 1652): Use of multiple types of snail evidenced by means of non-destructive imaging. *Microchem. J.* **126**, 515–523 (2016).
18. J. K. Delaney, D. M. Conover, K. A. Dooley, L. Glinsman, K. Janssens, M. Loew, Integrated X-ray fluorescence and diffuse visible-to-near-infrared reflectance scanner for standoff elemental and molecular spectroscopic imaging of paints and works on paper. *Herit. Sci.* **6**, 31 (2018).
19. H. Dubois, The Art of conservation XV. The conservation history of the Ghent Altarpiece. *Burlingt. Mag.* **160**, 754–765 (2018).
20. G. Van der Snickt, H. Dubois, J. Sanyova, S. Legrand, A. Coudray, C. Glaude, M. Postec, P. Van Espen, K. Janssens, Large-Area elemental imaging reveals Van Eyck's original paint layers on the Ghent Altarpiece (1432), rescoping its conservation treatment. *Angew. Chem. Int. Ed. Engl.* **56**, 4797–4801 (2017).
21. H. Dubois, Letter to the editor. *Burlingt. Mag.* **160**, 812 (2018).
22. E. M. Gifford, C. A. Metzger, J. K. Delaney, Jan van Eyck's annunciation. Painting materials and techniques, in *Fracture: Conservation, Science, Art History*, D. Barbour, E. M. Gifford, Eds. (National Gallery of Art, 2013), vol. 1, pp. 128–53.
23. R. Billinge, Examining Van Eyck's underdrawings, in *Investigating Van Eyck*, S. Foister, S. Jones, D. Cool, Eds. (Brepols, 2000), pp. 83–96.
24. T. Holger-Borchert, K. Jonckheere, M. Martens, D. Praet, P. Schmidt. Debat: Het onthulde Lam Gods, panel discussion, in *Ghent Altarpiece Second International Study Day* (September 11, 2018).
25. J. R. J. Van Asperen De Boer, A scientific re-examination of the Ghent Altarpiece. *Oud Holland* **93**, 141–214 (1979).
26. M. Martens, The creators. The role of Hubert and Jan van Eyck in the Ghent Altarpiece in *The Ghent altarpiece: Van Eyck: Art, History, Science and Religion*, D. Praet, M. Martens, Eds. (Hannibal, 2019), pp. 116–137.
27. M. Alfeld, K. Janssens, J. Dik, W. de Nolf, G. van der Snickt, Optimization of mobile scanning macro-XRF systems for the in situ investigation of historical paintings. *J. Anal. At. Spectrom* **26**, 899–909 (2011).
28. P. Van Espen, K. Janssens, J. Nobels, AXIL-PC, software for the analysis of complex X-ray spectra. *Chemospectroscopy Intell. Lab. Syst.* **1**, 109–114 (1986).
29. M. Alfeld, K. Janssens, Strategies for processing mega-pixel x-ray fluorescence hyperspectral data: A case study on a version of Caravaggio's painting *Supper at Emmaus*. *J. Anal. At. Spectrom* **30**, 777–789 (2015).
30. D. M. Conover, J. K. Delaney, M. H. Loew, Automatic registration and mosaicking of technical images of Old Master paintings. *Appl. Phys. A* **119**, 1567–1575 (2015).

Acknowledgments: The church wardens of cathedral of St. Bavo and their chairman L. Collin are acknowledged for the agreeable collaboration. We also wish to thank the other members of the conservation team of the *Ghent Altarpiece* (Royal Institute for Cultural Heritage, KIK-IRPA: B. Devolder, L. Mortiaux, M. Postec, F. Rosier, and G. Steyaert), the Museum of Fine Arts in Ghent as well as the members of the international committee. In addition, we thank C. Currie, head of the Documentation department of the KIK-IRPA, and her co-workers C. Fondaire, x-ray technician, and S. De Potter, IRR technician. We are indebted to E. A. Van Grevenstein-Kruse, J.K.D. and K.A.D. thank B. Devolder for help in collecting the

infrared RIS image data. **Funding:** This research was part of the activities of the Chair on Advanced Imaging Techniques for the Arts, established by the Baillet Latour fund. In addition, it was supported by the Belgian Science Policy Office (Project MO/39/011) and the Gieskes-Strijbis fund. We are also indebted to the BOF-GOA SOLARPaint project of the University of Antwerp Research Council and to FWO (Brussels) projects G056619N and G054719N. J.K.D. and K.A.D. acknowledge support from the National Gallery of Art. **Author contributions:** Data acquisition/analysis was performed by G.V.d.S., S.L., and K.J. (MA-XRF); K.A.D. and J.K.D. (infrared RIS); and J.S. (SEM-EDS and O.M.). Art historical interpretation of the data was performed by E.M.G. and H.D. The project was coordinated by H.D. along with G.V.d.S. and J.D. The manuscript was written by G.V.d.S., K.D., J.D., and E.M.G. with direct input from all other authors. All authors contributed to the manuscript. **Competing interests:** E.M.G. is a member of the International Commission for the Conservation of the *Ghent Altarpiece*. The other authors declare that they have no competing interests. **Data and**

materials availability: All data needed to evaluate the conclusions in the paper are present in the paper and/or the Supplementary Materials. Additional data related to this paper may be requested from the authors.

Submitted 19 February 2020

Accepted 16 June 2020

Published 29 July 2020

10.1126/sciadv.abb3379

Citation: G. Van der Snickt, K. A. Dooley, J. Sanyova, H. Dubois, J. K. Delaney, E. M. Gifford, S. Legrand, N. Laquiere, K. Janssens, Dual mode standoff imaging spectroscopy documents the painting process of the Lamb of God in the *Ghent Altarpiece* by J. and H. Van Eyck. *Sci. Adv.* **6**, eabb3379 (2020).

Dual mode standoff imaging spectroscopy documents the painting process of the Lamb of God in the *Ghent Altarpiece* by J. and H. Van Eyck

Geert Van der SnicktKathryn A. DooleyJana SanyovaHélène DuboisJohn K. DelaneyE. Melanie GiffordStijn LegrandNathalie LaquiereKoen Janssens

Sci. Adv., 6 (31), eabb3379. • DOI: 10.1126/sciadv.abb3379

View the article online

<https://www.science.org/doi/10.1126/sciadv.abb3379>

Permissions

<https://www.science.org/help/reprints-and-permissions>

Use of this article is subject to the [Terms of service](#)

Science Advances (ISSN 2375-2548) is published by the American Association for the Advancement of Science, 1200 New York Avenue NW, Washington, DC 20005. The title *Science Advances* is a registered trademark of AAAS.

Copyright © 2020 The Authors, some rights reserved; exclusive licensee American Association for the Advancement of Science. No claim to original U.S. Government Works. Distributed under a Creative Commons Attribution NonCommercial License 4.0 (CC BY-NC).